

NSLS-II STORAGE RING INSERTION DEVICE AND FRONT-END COMMISSIONING

G. Wang[#], T. Shaftan, C. Amundsen, G. Bassi, J. Bengtsson, A. Blednykh, E. Blum, W. Cheng, J. Choi, O. Chubar, T. Corwin, M. Davidsaver, L. Doom, W. Guo, D. Harder, P. He, Y. Hidaka, Y. Hu, P. Ilinski, C. Kitegi, S. Kramer, Y. Li, M. Musardo, D. Padrazo, B. Podobedov, K. Qian, R. Rainer, J. Rank, S. Seletskiy, S. Sharma, O. Singh, V. Smaluk, R. Smith, T. Summers, T. Tanabe, F. Willeke, L. Yang, X. Yang, L. Yu, BNL, Upton, NY 11973, USA

Abstract

The National Synchrotron Light Source II (NSLS-II) is a state of the art 3 GeV third generation light source at Brookhaven National Laboratory. During spring/ summer of 2014, the storage ring was commissioned up to 50 mA without insertion devices. In the fall of 2014, we began commissioning of the project beamlines, which included seven insertion devices on six ID ports. Beamlines IXS, HXN, CSX-1, CSX-2, CHX, SRX, and XPD-1 consist of elliptically polarized undulator (EPU), damping wigglers (DW) and in-vacuum undulators (IVU) covering from VUV to hard x-ray range. In this paper, experience with commissioning and operation is discussed. We focus on reaching ring storage ring performance with IDs, including injection, design emittance, compensation of orbit distortions caused by ID residual field, source point stability, beam alignment and tools for control, monitoring and protection of the ring chambers from ID radiation.

INTRODUCTION

The National Synchrotron Light Source II (NSLS-II) is a 3 GeV, ultra-small emittance (1 nm-rad), high brightness ($>10^{21}$ photons s^{-1} mm^{-2} $mrad^{-2}(0.1\%BW)^{-1}$) third generation light source [1]. It can support 60~80 beamlines stemming from insertion devices, three pole wigglers and bending magnets. The storage ring (SR) commissioning took about two months and reached and exceeded key performance parameters (KPP were 25 mA at 3 GeV of the beam energy) with superconducting RF cavity during July 2014 [2-4]. Once the start-up goals were accomplished we moved to phase-I insertion devices commissioning. The insertion device (ID) and their front end (FE) commissioning commenced in Oct., 2014 and took about 2 months for all the project IDs so that the beamline commissioning with the beam began in Dec. 2014. Since then all installed IDs operate routinely supplying light for the NSLS-II users at the level of 50 mA of circulating current.

NSLS-II design is based on 30 cells of double-bend-achromat lattice, including 15 long straight sections (9.3 m) and 15 short straight sections (6.6 m). The IDs [5] location and their main parameters are listed in Table 1.

In this paper we describe the results of the ID commissioning including compensation of their effects on closed orbit, perturbation of linear optics, optimization of emittance and injection efficiency, as well as the ID

source point alignment along the front-ends, testing of equipment protection system and reaching high beam stability.

Table 1: NSLS II Phase I IDs Main Parameters

Beam Line	Type	L [m]	λ [mm]	K_{max}	Gap [mm]
CSX1/ CSX2	EPU49	4	49	2.6 (heli)	11.5
				4.3 (Lin)	
				3.2 (vlin)	
				1.8 (45d)	
IXS	IVU22	3	22	1.52	7.4
HXN	IVU20	3	20	1.83	5.2
CHX	IVU20	3	20	1.83	5.2
SRX	IVU21	1.5	21	1.79	6.4
XPD/ PDF	DW100	6.8	100	~16.5	15.0

ID COMMISSIONING

Changing ID gaps affects stored beam closed orbit, perturbs linear optics (inducing tune shift and beta beat), reduces injection efficiency. All project IDs were commissioned in several steps: 1) aligning beam orbit in an ID with the stored beam in low current, (along with the ID elevation adjustment if available); 2) measuring ID field integrals and minimizing related orbit distortions by setting fields in the ID trim coils (usually the latter took several iterations so to reach residual distortions on the $\sim\mu m$ level); 3) collect correction ID coil currents into a single lookup table and interpolate the measured values for a range of gaps; 4) measure the optics distortion at different gaps and correct them distortion by comparing with the ideal model; 5) assess and optimize ID impact on the injection efficiency.

Close Orbit Perturbation and Compensation

The ID impact on the beam dynamics in the first order comes from the non-zero 1st and 2nd residual magnetic field integrals. These integrals introduce local orbit position and angle shifts and lead to closed orbit distortion. This effect is local and is compensated by the ID trim coils, installed on both ID ends.

The closed orbit change as a function of the ID gap is on the order of 20 μm rms for the IVUs, 40 μm rms for the EPU and 150 μm rms for DWs. After the first iteration, the rms value of residual orbit is corrected to <5 μm . After a few iterations, the final residual orbit rms value is under 2 μm .

[#]gwang@bnl.gov

Figure 1 shows one DW effect on the close orbit without and with trim coil compensation. The fitted field integrals retrieved from the measured orbit distortion are within the specification. The correlation between beam based measurement and magnetic measurement was found to be poor, several possible causes have to be investigated such as, orientation difference between lab and tunnel installation or the background. In the horizontal plane, the trim coils can compensate closed orbit distortion quite well. However, in the vertical plane, the trim coils are under designed and capable of correcting closed orbit to the level of $\sim 10 \mu\text{m}$, far from what is required for compensation of the ID effects. Thus we established lookup table via using two regular storage ring correctors located around the IDs instead of using the ID vertical correction coils.

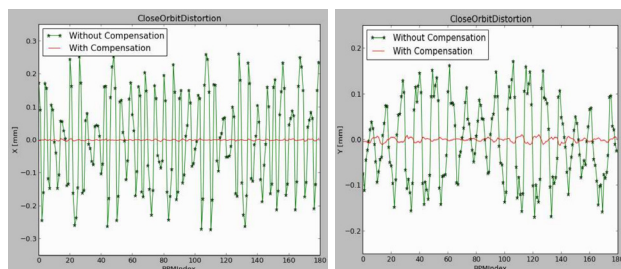


Figure 1: DW effect on close orbit without and with compensation.

Linear Optics Perturbation and Compensation

The tune shift and linear optics distortion driven by IVUs and EPU are negligible. The measured vertical tune shift agrees well with model, as shown in Figure 2.

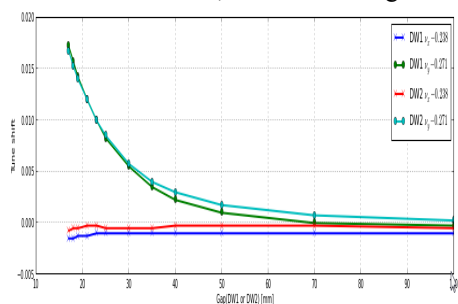


Figure 2: DW effect on vertical tune shift.

Aside from vertical tune shift, damping wigglers produce substantial beta-beat in the vertical plane. We used two methods to compensate for the beta-beat effect. First method was in matching local optics distortion with three pairs of quads bounding DWs, and then corrects tunes using all SR quadrupoles. The other way is to use BPM turn-by-turn data to measure the beta beat and correct it with the DW ideal model, together with correcting tunes, using all SR quadrupoles. Both methods proved to work quite well. After the optics correction, the beta-beat was reduced from 6.5% to 3.0% as shown in Figure 3.

We created various lookup table as a function of the ID gap using ideal model.

ID Effect on Injection Efficiency

We observed no significant impact on injection efficiency from all IDs except for C5 IVU. Figure 4 shows that when the gap is $< 10 \text{ mm}$, the ID leads to reduction of the injection efficiency. At the minimum gap of 6.25 mm, the storage ring was not able to capture the beam. As we found out this was an alignment problem, caused by a misalignment of about 0.7 mrad. After realignment, the injection efficiency was observed as good as for the IVU C5 ID with the gap open.

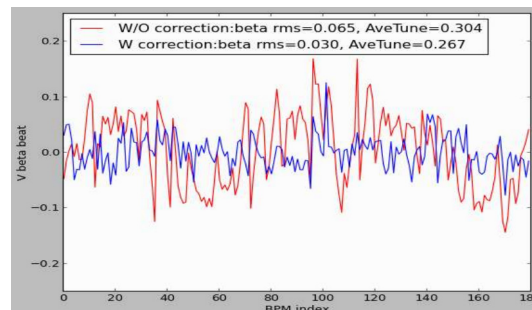


Figure 3: DW effect on vertical plane beta beat without and with optics compensation.

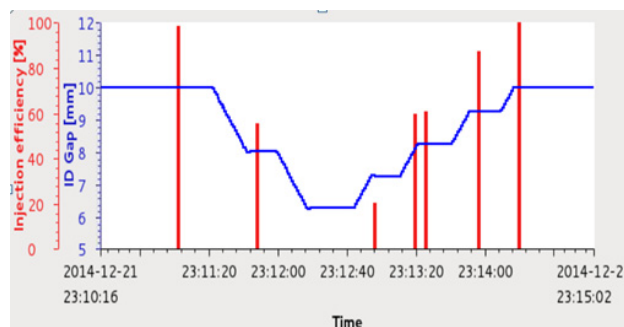


Figure 4: C5 IVU effect on the injection efficiency.

At the NSLS-II the SR lattice is designed to deliver the horizontal emittance of 2.2 nm rad. The compliment of 3 x 2 damping wigglers produce additional damping and furthermore reduce the beam emittance to the design value of 1 nm rad.

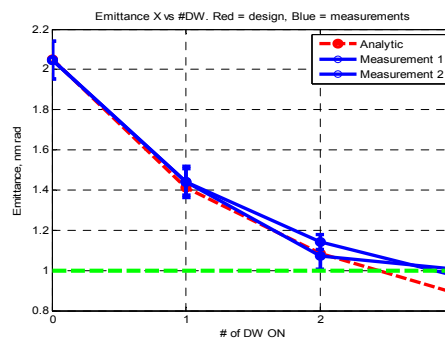


Figure 5: Experimental results (blue for two sets of measurements) vs theoretical estimation. Green line: the project goal of 1 nm.

We carried out two sets of beam size measurements [6] at the beam current of 1.5 mA. We used X-ray diagnostics aimed at the bending magnet synchrotron radiation

through a pin hole for the beam size measurements. The source point is located at the entrance of the first bending magnet (BM-A) in the DBA achromat, with near-zero dispersion. The horizontal emittance value was retrieved using the design value of the beta-function. Figure 5 demonstrates the outcome of our experiments indicating good agreement with expectations and demonstrating the project goal of 1 nm-rad emittance in the horizontal plane.

BEAM STABILITY

We specified stability of the NSLS-II beam at the 10% of beam sizes in the source points (centres of IDs). This tight constraint is important for the NSLS-II X-ray imaging experiments. Figure 6 shows the beam orbit motion relative to the beam size without and with fast orbit feedback (FOFB). In the X plane, the orbit stability has been measured to be below 1% of X-beam size even without FOFB. In the Y-plane, the orbit stability is 20% of beam size without FOFB and recently reached the specification with FOFB.

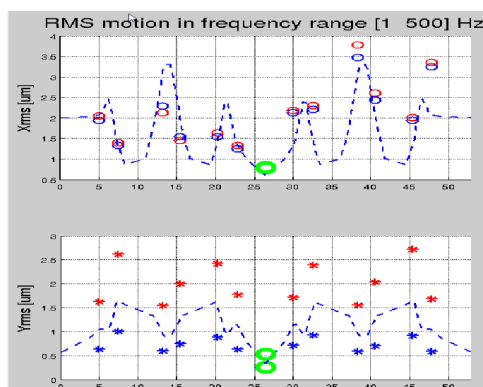


Figure 6: beam orbit stability without and with fast orbit feedback (Blue/red: FOFB on/Off, Dash line: 1% X and 10% Y beam size).

FRONT END COMMISSIONING

Commissioning of the NSLS-II Storage Ring Front-Ends (FE) consists of the two main tasks. The first task is to align synchrotron radiation fan (SRF) from the insertion device (ID) with respect to the FE components. The second task is commissioning of the Active Interlock (AI) system.

A typical FE contains fixed mask aperture, which trims the SRF to the level acceptable for the rest of the FE and along the respective beamline. One of the most useful diagnostic tools for SRF alignment is the FE insertion flag that we developed and installed right after the fixed mask.

We followed this procedure for SRF alignment. First, the e-beam was centered through dedicated ID BPMs. Next, we closed the ID gap to the value corresponding to K_{ID} was of the order of unity. Using the FE flag we observed a round spot induced by SRF and the shadows imposed by the fixed mask. Finally, by creating angular deflection of the e-beam orbit we scanned the fixed mask with the SRF and found local e-beam orbit settings

centering the SRF both with respect to the ID axis and in the fixed mask. Since the rest of the FE components were well surveyed with respect to the fixed mask, the procedure above worked well for aligning the SRF through the FE.

The Active Interlock (AI) system has been designed to protect the storage ring vacuum chambers, FE and beamline components from the damage by SRF. We limited the beam orbit to stay within the AI envelope (AIE) at beam current exceeding 2 mA. Detailed functional tests on the AI were performed prior to FE commissioning. During the AI commissioning we lowered the beam current and intentionally created various fault conditions to test AI response [7].

CONCLUSION

Project beamline IDs and front-ends have been successfully commissioned and brought to the user operations with the circulating current up to 50 mA.

We compensated ID impact on the beam orbit down to the um level by measuring and optimizing ID gap lookup tables. Injection efficiency with all ID gaps closed is comparable with injection into the bare lattice (above 95%). Reduction of the beam emittance with the damping wiggler gaps closed agreed with theoretical estimates. Thus the goal of the NSLS-II design (emittance of <1nm-rad) has been reached. The NSLS-II Fast Orbit Feedback helped to stabilize beam orbit within 10% of beam sizes.

During the FE commissioning we aligned the synchrotron radiation fan using X-ray flags. Active interlock system is developed, tested and engaged. We are developing a post-mortem capability for the NSLS-II controls to diagnose cause of the AI trips.

REFERENCES

- [1] F.J. Willeke, TUOBS3, Proc. of PAC'11, New York, USA (2011); <http://www.JACoW.org>
- [2] G. Wang, "Results of the NSLS-II commissioning," presented at the APS April Meeting 2015, Bulletin of the American Physical Society **60**(4), Abstract: M12.00002 (2015).
- [3] F. Willeke, "Commissioning Results of NSLS-II," MOYGB3, these proceedings, Proc. of IPAC15, Richmond, VA, USA (2015); <http://www.JACoW.org>
- [4] G. Wang et al., NSLS II Commissioning Report. BNL Tech. Note 168.
- [5] M. Musardo et al., "Magnetic Measurements of the NSLS-II Insertion Devices," TUPJE037, these proceedings, Proc. of IPAC15, Richmond, VA, USA (2015); <http://www.JACoW.org>
- [6] T. Shaftan et al., NSLS-II Emittance and Lifetime with Damping Wigglers, BNL Tech. Note 157.
- [7] S. Seletskiy et al., "Commissioning of Active Interlock System for NSLS II Storage Ring," TUPMA057, these proceedings, Proc. of IPAC15, Richmond, VA, USA (2015); <http://www.JACoW.org>